Available online at www.sciencedirect.com
SCIENCE DIRECT®
Journal of Sound and Vibration 288 (2005) 669–699
JOURNAL OF SOUND AND VIBRATION
www.elsevier.com/locate/jsvi

Vibro-acoustic analysis of complex systems

P.J. Shorter*, R.S. Langley[1]

ESI US R&D Inc., 12555 High Bluff Drive, Suite 250, San Diego, CA 92130, USA

Accepted 5 July 2005
Available online 2 September 2005

Abstract

A general method is presented for predicting the ensemble average steady-state response of complex vibro-acoustic systems that contain subsystems with uncertain, or random, properties. The method combines deterministic and statistical techniques to produce a non-iterative hybrid method that incorporates equations of dynamic equilibrium and power balance. The method is derived explicitly without reference to statistical energy analysis (SEA); however, it is seen that the wave approach to SEA can be viewed as a special case of the proposed method. The proposed method provides a flexible way to account for necessary deterministic details in a vibro-acoustic analysis without requiring that an entire system be modeled deterministically. The method therefore provides a potential solution to the mid-frequency problem (in which a system is neither entirely deterministic nor entirely statistical). The application of the method is illustrated with a numerical validation example.

1. Introduction

This paper is concerned with the development of a predictive method for describing the transmission of noise and vibration in complex structural-acoustic systems. The term 'complex' is used to indicate that the properties of certain subsystems of a system are not known to a high-enough level of precision to justify (or warrant) the use of a deterministic analysis. Such

*Corresponding author. Fax: +1 858 350 8328.
E-mail address: pjs@esi-group-na.com (P.J. Shorter).
[1]Permanent address: Department of Engineering, University of Cambridge, Trumpington Street, Cambridge CB2 1PZ, UK.

0022-460X/$ - see front matter © 2005 Elsevier Ltd. All rights reserved.
doi:10.1016/j.jsv.2005.07.010

subsystems typically support several propagating wavetypes (with many directions of propagation) and are large in comparison with a wavelength. The traditional approach to describing the dynamic interactions of such subsystems is to use the method of statistical energy analysis (SEA) [1,2].

Broadly speaking, SEA represents a field of study in which statistical descriptions of a system are employed in order to simplify the analysis of complicated structural-acoustic problems [3]. While such a definition encompasses many different methods and analysis techniques, SEA is often perceived (perhaps for historical reasons) as being a method for describing the storage and transfer of vibrational energy between subsystems of weakly coupled modes. In particular, the energy storage capacity of a given subsystem is described by a parameter termed the modal density; the coupling between subsystems is described by parameters termed coupling loss factors (CLFs). Applying conservation of energy to each subsystem then results in a set of linear simultaneous equations for the subsystem energies.

The initial justification for the SEA equations was based on studies of the energy flow between pairs of coupled oscillators. The implicit assumptions associated with the extension of the two-oscillator result to sets of coupled oscillators (the 'modal' approach to SEA) has been the subject of much discussion over the past 40 years (see Fahy [2], for example). It is perhaps fair to conclude that while providing physical insights into the response of certain systems, the modal approach remains qualitative in nature and (for structural problems) does not provide a practical method for calculating the parameters used in an SEA model. Most analytical predictions of the SEA parameters are based on a wave approach. In the wave approach to SEA, a complex subsystem is represented as a collection of propagating wavetypes. The energy storage capacity of a given subsystem is related to the expected group velocity and dimension of the subsystem. The CLFs at a given junction are found by calculating the local transmission of energy into the 'direct fields' of a number of receiving subsystems, due to the presence of a 'diffuse reverberant field' (with a specified energy density) in an excited subsystem. The terms 'direct field' and 'diffuse reverberant field' are widely used, but their definition is often qualitative and difficulties can arise when applying such concepts to general junctions (this point is discussed in more detail in the following section).

The wave approach to calculating the SEA CLFs for line junctions was initially discussed by Lyon and Eichler [4] (the approach appears to have been motivated in part by Heckl's demonstration that room acoustics concepts could be successfully applied to structural problems [5]). For line junctions, a diffuse field is interpreted as a set of uncorrelated plane waves with random headings and equal power. A wave-scattering problem is then formulated and wave transmission coefficients obtained for various discrete angles of incidence (as illustrated in Fig. 1a). The plane-wave approach for calculating the CLFs between line-connected subsystems has changed little over the past 40 years. The advent of dynamic stiffness-based calculations of the wave transmission coefficients between arbitrarily oriented plate subsystems has, however, substantially increased the types of junction that can be modeled (see, for example, Langley and Heron [6] and Bosmans and Nightingale [7]).

The plane-wave approach provides a good description of the CLFs of junctions that are planar and large in comparison with a wavelength. Based on the widespread use of this approach, one might perhaps assume that plane waves are fundamental to the wave approach to SEA. However, this is not the case. Consider, for example, a compact point junction between a plate and a

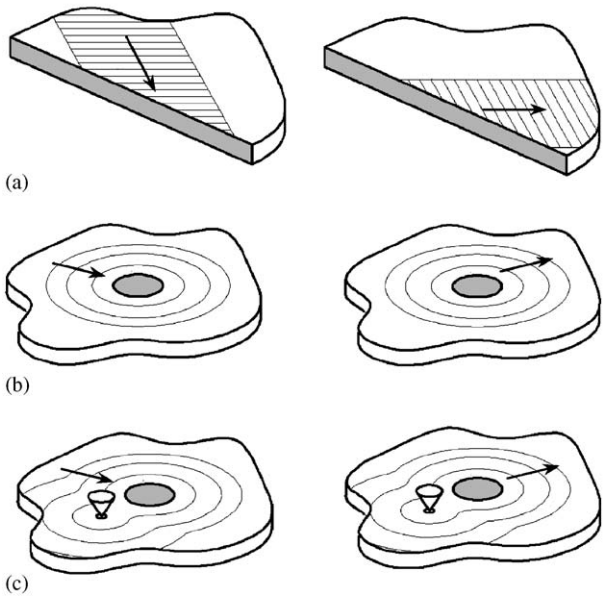

Fig. 1. Illustration of the 'natural' wavetypes used to describe a "diffuse reverberant field" (left) and "direct field" (right) for: (a) line, (b) point and (c) general connections.

cantilevered beam. Excitation of the beam results in the generation of outgoing cylindrical waves in the plate. In principle, such cylindrical waves can be described in terms of a large number of coherent plane waves. However, such a description is awkward; plane waves do not provide a 'natural' basis for describing the direct field of the plate. The most natural coordinates for describing the direct field of the plate are clearly cylindrical waves (as illustrated in Fig. 1b). However, it is not immediately obvious what properties should be ascribed to a set of incident cylindrical waves in the plate in order to describe a diffuse reverberant field. It transpires that a diffuse field can be described in terms of cylindrical waves [8] and this result may be used to calculate CLFs for compact point junctions [9]. Based on this example, one can conclude that the most natural wave description for the direct and reverberant fields of an SEA subsystem varies depending on the subsystem and connection of interest.

Consider now the problem of describing the energy flows through the connection to the plate subsystem illustrated in Fig. 1c. A single deterministic boundary condition is located within a few wavelengths of the connection. The presence of the boundary condition has a large influence on the local impedance of the connection. In turn, this affects the energy flow through the connection (and the CLFs associated with any junctions which involve the connection). However, it is not immediately obvious how the boundary condition can be accounted for in the traditional wave approach to SEA. Firstly, it is not obvious what the most natural wavetypes are for describing the plate response. One could, for example, describe the response in terms of the coherent response of a large number of cylindrical waves. Such a description is, however, awkward; cylindrical waves do not provide a 'natural' basis for describing the direct field of this connection. Secondly, it is not immediately obvious how a diffuse reverberant field should be interpreted for such a connection.

This example suggests that a more general definition of a 'direct field' and 'diffuse reverberant field' is required in order to use the wave approach to SEA to calculate the CLFs for general junctions.

The example presented in Fig. 1c is a specific instance of a more general problem encountered in SEA, which occurs when deterministic boundaries of a subsystem lie within a few wavelengths of a connection. The frequency and/or ensemble average flow of energy through a junction between a set of coupled subsystems depends on: (i) the local impedance of the junction and (ii) the local impedance of each connected subsystem. The local junction impedance depends on the detailed construction of the junction and is, for example, sensitive to whether the junction contains isolators or stiffeners. In general, a detailed description of the impedance of a complex junction requires a detailed local deterministic model of the junction (based on, for example, a local finite element model).

The local impedance of a connection to a (two- or three-dimensional) subsystem is typically sensitive to the deterministic details of the subsystem that lie within a few wavelengths of the connection. For subsystems that are large compared with a wavelength, one can often obtain a sufficiently precise description of the frequency and/or ensemble average subsystem impedance by considering the impedance of the equivalent semi-infinite subsystem. However, for subsystems that are small compared with a wavelength, the entire boundary of the subsystem lies 'within a few wavelengths of the connection'. Such subsystems often exhibit strongly coherent behavior across a broad frequency range and can cause distinct fluctuations in the broadband frequency response of a system (the coherence referred to here describes the coherence across a frequency band or across an ensemble). The impedance seen from the junction depends on the details of the entire subsystem; an accurate description of the local connection impedance therefore typically requires that the entire subsystem be modeled deterministically.

To clarify ideas, it is helpful to consider the specific example of the transmission of vibrational energy between the three plates illustrated in Fig. 2. Each plate can undergo both out-of-plane flexural motion and in-plane stretching and shear motion. Typically, the flexural motion will have a much shorter wavelength of deformation than the two in-plane motions. For example, the wavelengths of flexural, shear and extensional waves within a 1-mm-thick steel plate at 1 kHz are (approximately) 0.1, 3.2 and 5.5 m, respectively. For many structures of practical interest, there

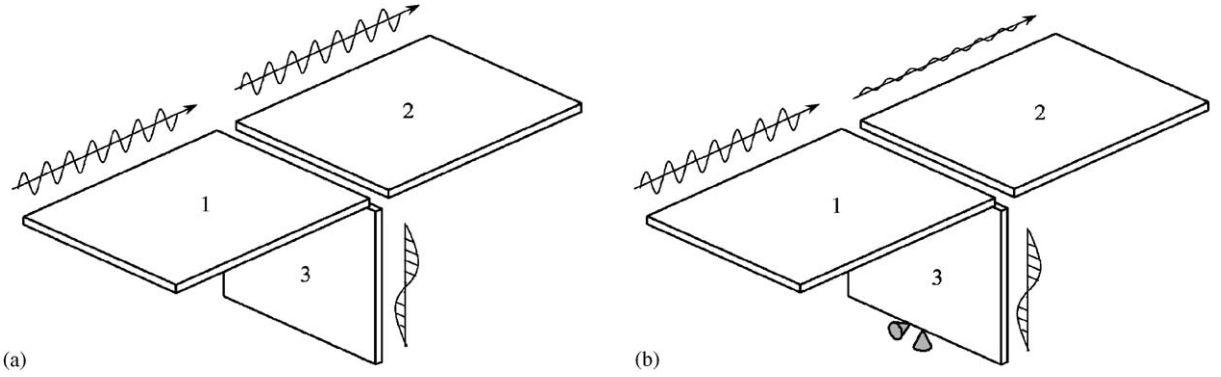

Fig. 2. Flexural wave transmission between subsystems 1 and 2 is sensitive to the in-plane boundary impedance applied to a 'distant' boundary of subsystem 3. Case (a) represents a free boundary, case (b) represents a partially clamped boundary.

exists a fairly broad frequency range in which a plate subsystem is large in comparison with a flexural wavelength, yet small in comparison with the in-plane wavelengths. The short-wavelength motion is very difficult to model deterministically, partly because many degrees of freedom are required to capture the detailed deformation pattern, and partly because the motion is very sensitive to any imperfections in the system, so that no two nominally identical structures will have exactly the same response. In contrast, the long-wavelength motion is often difficult to describe in the traditional wave approach to SEA.

Consider, for example, the calculation of the SEA CLF between the flexural wavefields of plates 1 and 2 illustrated in Fig. 2. If all subsystems are large compared with a wavelength, then the transmission of energy through the junction is determined by the local properties of the subsystems (and wavefields) in the vicinity of the junction. The traditional wave approach to SEA (based on the impedances of the equivalent semi-infinite subsystems) typically provides a good estimate of the CLFs for the junction. However, if any of the subsystems connected to the junction are small compared with a wavelength, then the transmission of energy through the junction is typically no longer governed by the local junction properties. For example, Fig. 2 illustrates how the CLF between the flexural wavefields of plates 1 and 2 is sensitive to the in-plane impedance applied to a 'distant' boundary of subsystem 3. In Fig. 2a, the distant boundary is unconstrained and (below the first in-plane resonance) the in-plane impedance seen at the junction is mainly governed by the mass of plate 3. In Fig. 2b, a single point on the distant boundary is clamped. The in-plane impedance seen at the junction (below the first in-plane resonance) then depends on the membrane stiffness of plate 3. The two different in-plane impedances can cause significant differences in the way in which flexural waves are scattered at the junction. An accurate description of the in-plane impedance of plate 3 seen by the junction typically requires a deterministic finite element description of the membrane behavior of the plate.

In summary, in many instances a general description of the ensemble and/or frequency average energy flows between a set of coupled subsystems often requires that certain parts of a system be described deterministically. A general method for introducing an arbitrary amount of deterministic detail into an SEA model, along with a general method for calculating the CLFs between SEA subsystems, is not currently available. The lack of such a method has been referred to previously as the 'mid-frequency' problem (although the term 'strong coupling' has also been used to refer to certain aspects of this problem [10]). This paper provides a potential solution to the mid-frequency problem. A general method is presented for predicting the ensemble average response of complex vibro-acoustic systems with uncertain properties. The approach is derived explicitly without reference to existing SEA methods. However, it is shown that the traditional wave approach to SEA can be viewed as a special case of the more general method. The advantages and limitations of the approach are discussed and numerical validation examples are presented.

2. A complex vibro-acoustic system

2.1. Terminology

Consider the vibro-acoustic system illustrated in Fig. 3. The system consists of a number of coupled subsystems excited by a spatially distributed load. Each subsystem consists of a domain Ω

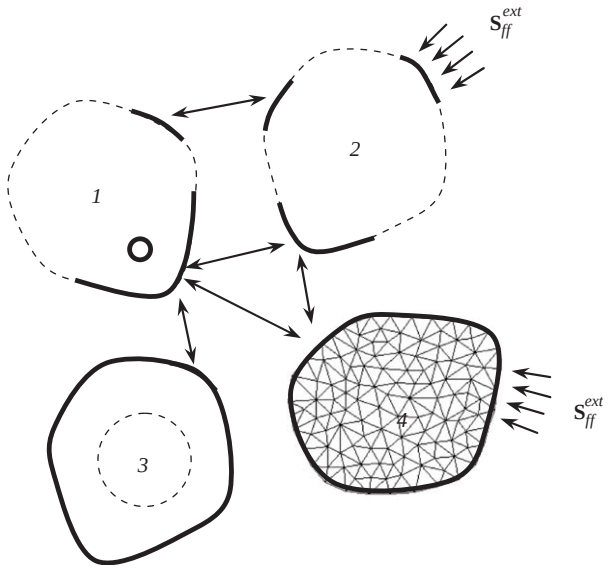

Fig. 3. A system that comprises of a number of coupled subsystems: solid line indicates deterministic boundary, dashed line indicates random boundary, double arrow indicates a junction, single arrow indicates a distributed excitation (mesh used to indicate that a subsystem is entirely deterministic).

and a boundary Γ. In what follows, the domain is assumed to be a three-dimensional volume (although this volume may be defined implicitly by, for example, the two-dimensional neutral surface of a plate and an associated thickness). At the excitation frequency of interest, some of the subsystems may exhibit very short-wavelength deformation, while others may have a relatively long wavelength of deformation. The boundary of the subsystems need not be simply connected and the subsystems may therefore contain holes, cutouts and internal discontinuities.

It is assumed that certain regions of the boundary of each subsystem can be identified whose properties are known precisely. Such regions are referred to as the 'deterministic boundary' regions of a subsystem. Any remaining regions of the boundary are assumed to be very uncertain and are termed the 'random boundary' regions of a subsystem. Regions of the boundary that allow energy to be transferred into or out of a subsystem (due to external excitations or coupling to adjacent subsystems) are termed 'connection regions'. It is assumed that the connection regions of a subsystem form part of the deterministic boundary. For example, the deterministic boundary might be defined to be the region of the boundary that lies within a few wavelengths of each of the connection regions of a subsystem (in a given frequency range of interest).

If the deterministic boundary of a subsystem contains various non-contiguous connection regions, then the relative locations of any two connection regions to the same subsystem can either be: (i) known precisely or (ii) unknown. In the former case the connection regions to a subsystem are said to be 'coherently coupled', in the latter case the connection regions to a subsystem are said to be 'incoherently coupled'. Typically, connection regions which lie within a few wavelengths of each other are assumed to be 'coherently coupled', while connection regions that are separated by several wavelengths are assumed to be 'incoherently coupled'. In some instances, the

deterministic boundary of a subsystem might represent the entire subsystem boundary; the subsystem is then said to be 'deterministic'. Subsystems which are not deterministic are said to be 'statistical'.[2]

The connection regions of different subsystems are coupled together by various 'junctions'. Each junction typically involves several connection regions. In what follows, it is assumed that all connection regions associated with a given junction are coincident and have compatible displacement fields. The junctions can be separated into three types: (i) those that involve only deterministic subsystems, (ii) those that involve only statistical subsystems, and (iii) those that involve a mix of deterministic and statistical subsystems. These junctions are referred to as: (i) deterministic junctions, (ii) statistical junctions and (iii) hybrid junctions, respectively. It can be noted that the term 'statistical junction' is abbreviated terminology for 'a junction between statistical subsystems'.

To clarify the previous terminology (and the notion of a random boundary), it is perhaps helpful to consider a number of simple examples. Consider a system that comprises of a small stiff panel located in the window of a large reverberant chamber. Across the frequency range of interest the panel may contain relatively few half wavelengths, while the reverberant chamber may contain many half wavelengths. Such a system may be described using two subsystems: a panel subsystem and a large acoustic cavity subsystem. The panel occupies a three-dimensional volume of space, each dimension of which is small compared to (or commensurate with) the wavelengths of deformation within the panel. One might therefore choose to define the deterministic boundary of the panel subsystem as the entire exterior boundary surface of the panel. If the panel does not contain any internal boundaries (associated with, for example, random discontinuities embedded within the panel), then all boundaries of the panel are deterministic and the panel is therefore said to be a 'deterministic subsystem'.

The exchange of energy between the panel and cavity occurs through one face of the panel (the 'wetted' face of the panel). One can therefore define connection regions for both the panel and cavity subsystems (in this example, the connection region represents a rectangular area with known dimension). Consider now the definition of the deterministic boundary for the cavity subsystem. As discussed previously, the connection regions of a subsystem must form part of the deterministic boundary. Furthermore, the boundaries of the chamber that lie within a few acoustic wavelengths of the connection region can also be assumed to form part of the deterministic boundary. The deterministic boundary for the cavity then consists of the connection region and a 'deterministic baffle' that lies within a few wavelengths of this connection region (for a typical reverberant chamber one might, for example, specify that the reverberant chamber has rigid walls in the vicinity of the connection and that the window in which the panel is placed is recessed with a particular geometry).

If information is available for the overall dimensions of the chamber (and the geometry and location of any internal diffusers within the chamber), one might perhaps be tempted to include such information in the description of the deterministic boundary of the cavity. However, if the dimensions of the cavity are large compared with a wavelength, then it is likely that such dimensions will not be known with sufficient precision to be described deterministically. It is

[2]The terms 'SEA subsystem', 'complex subsystem' or 'fuzzy subsystem' are perhaps equally applicable in the current context [3].

therefore more convenient to instead assume that all remaining boundaries of the cavity form part of an (unspecified) random boundary. Since the entire boundary of the cavity subsystem has not been defined deterministically, the cavity is said to be a 'statistical subsystem'. The junction between the connection regions of the panel and cavity couples deterministic and statistical subsystems and is therefore termed a 'hybrid junction'.

Consider now an example in which *two* panels are located in two separate windows in the previous reverberant chamber as illustrated in Fig. 4. If the connection regions of the two panels are within a few wavelengths of each other, then the two panels are likely to exhibit coherent interactions with each other. The two connection regions for the cavity may therefore be said to be 'coherently coupled'. If, however, the precise locations of the two connection regions are large compared with a wavelength, the coherent interaction between the two connection regions is likely to be sensitive to perturbation; the two connection regions may therefore be said to be 'incoherently coupled'.

For many structure-borne noise problems, a given subsystem may be entirely surrounded by connection regions. Consider, for example, a thin rectangular plate whose edges are connected to a stiff beam framework as illustrated in Fig. 5. Across the frequency range of interest, the beams may exhibit long-wavelength behavior (which is best represented deterministically) while the flexural wavefield of the plate may exhibit short-wavelength behavior (which is best represented statistically). However, since the external boundary of the plate subsystem is composed entirely of connection regions, one might conclude (based on the previous discussion) that the plate must be modeled as a deterministic subsystem. However, this is not the case. The random boundary may, for example, represent a series of hypothetical curves contained within the subsystem which denote the presence of uncertainties within the subsystem. The location and geometry of the

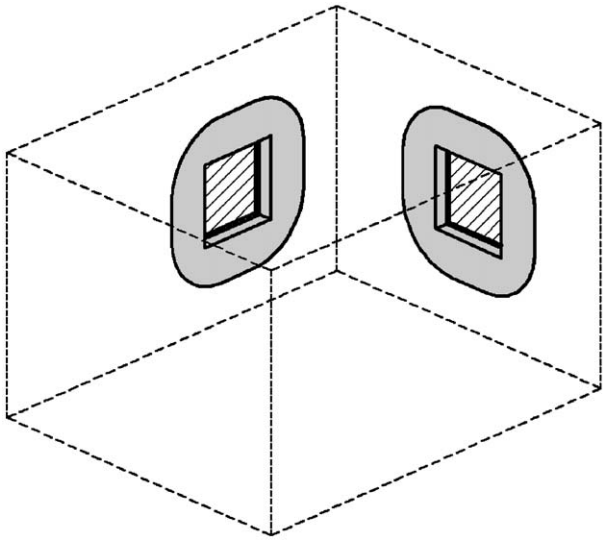

Fig. 4. Example of two stiff panel subsystems located in windows in a large reverberant chamber. Shaded region indicates deterministic boundary assumed for cavity subsystem; cross-hatched region indicates connection regions for cavity subsystem.

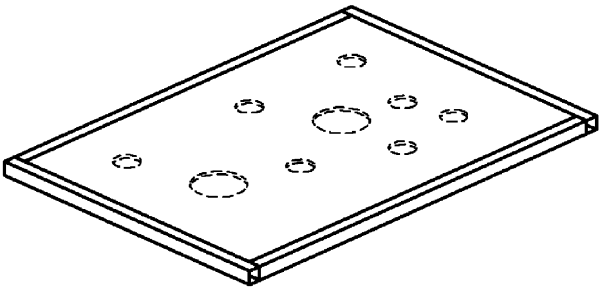

Fig. 5. Example of a statistical plate subsystem with an external deterministic boundary (solid lines) and a series of hypothetical internal random boundaries (dashed lines).

random boundary need *not* be specified in the present analysis—it is sufficient to note that such boundaries exist and act as a random scattering device in each statistical subsystem. Various approaches then exist for describing the response of the plate. For example, if the dimensions of the plate are large compared with a wavelength then one approach is to define four separate connection regions, one for each edge of the plate, and assume that the different connection regions are 'incoherently coupled'. The development of such an approach (and an investigation of its accuracy) will be reported in a separate publication.

2.2. Degrees of freedom

A set of generalized coordinates with degrees of freedom $\mathbf{q}_1$ can be chosen to describe the displacement response of the deterministic subsystems. The degrees of freedom may, for example, represent nodal or modal degrees of freedom of the deterministic subsystems. It is assumed in what follows that the basis function associated with each generalized coordinate is real-valued. As discussed previously, the displacement fields of the various connection regions associated with a given junction are assumed to be compatible. The degrees of freedom $\mathbf{q}_1$ therefore also describe the displacement fields across the 'deterministic' and 'hybrid' junctions. In order to describe the displacement field across the 'statistical' junctions in a model, it is necessary to define an additional set of generalized coordinates with degrees of freedom $\mathbf{q}_2$. These degrees of freedom may, for example, represent the nodal degrees of freedom of a surface mesh (or, for planar connections, they may represent trace wavenumbers or terms in a Fourier series).

The degrees of freedom $\mathbf{q}_1$ and $\mathbf{q}_2$ may be combined to form a single set of degrees of freedom $\mathbf{q}$, where $\mathbf{q} = \left[\mathbf{q}_1^{\mathrm{T}} \quad \mathbf{q}_2^{\mathrm{T}}\right]^{\mathrm{T}}$. The degrees of freedom $\mathbf{q}$ are deterministic and fully define the displacement field across all deterministic subsystems and across all connection regions within a system. Fig. 6 illustrates the definition of the degrees of freedom $\mathbf{q}_1$ and $\mathbf{q}_2$ for a simple example system consisting of three coupled plates (two statistical plates and one deterministic plate). The displacement response across the deterministic plate is described by the degrees of freedom $\mathbf{q}_1$, while the displacement response across the junction between the two statistical plates is described by the degrees of freedom $\mathbf{q}_2$.

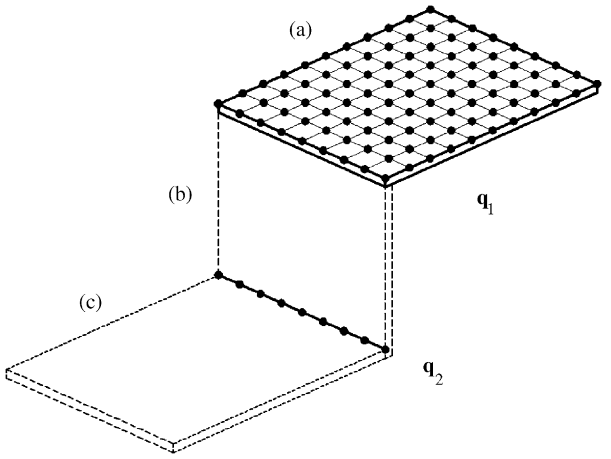

Fig. 6. Degrees of freedom q_1 and q_2 used to describe response of deterministic subsystem (a) and junction between statistical subsystems (b) and (c).

The contribution to the global dynamic stiffness matrix arising from the deterministic subsystems can be obtained at a given frequency of interest ω (using, for example, a finite or boundary element model), and written as $\mathbf{D}_d(\omega)$. In general, the deterministic subsystems will be non-conservative and the dynamic stiffness matrix $\mathbf{D}_d(\omega)$ will therefore be complex. The uncoupled equations of motion for the deterministic subsystems can then be written as

$$\mathbf{D}_d\mathbf{q} = \mathbf{f}_d. \tag{1}$$

where $\mathbf{f}_d$ is a vector of generalized forces applied to the deterministic degrees of freedom $\mathbf{q}$.

2.3. The direct and reverberant fields of a statistical subsystem

Consider now the problem of describing the response of the statistical subsystems in the system. In principle, one could adopt a similar approach to the previous section and attempt to calculate the 'exact' contribution to the global dynamic stiffness matrix arising from each statistical subsystem. However, an exact description of the dynamic behavior of such subsystems requires that the properties of the subsystems are known 'exactly'. In practice, such information is seldom available and there is therefore an unavoidable amount of uncertainty (or missing information) associated with the properties of such subsystems.

Various approaches exist for accounting for this missing information. One approach is to assume arbitrary properties for the missing information. Such an approach is adopted (albeit implicitly), when a deterministic model is used to describe the response of a complex system at higher frequencies. The main drawback with such an approach (leaving aside issues of computational expense) is that one is never quite sure how sensitive the computed response is to the information that was 'made up'. Erroneous assumptions about the properties of a system can lead to erroneous conclusions about its response.

An alternative approach is therefore to account for the missing information by adopting a statistical description of the subsystem dynamic behavior. A question then arises as to how one

should define the statistical properties of the uncertain subsystems. The classical approach to this problem is to specify the subsystem properties in terms of a detailed joint probability density function. Various analytical and numerical methods can then be employed to relate the probability density of the input parameters to the probability density of the response. The main drawback with such an approach (leaving aside issues of precision and computational expense) is that the definition of the detailed joint probability density function requires more information about the subsystem not less. From a qualitative point of view, such methods require an extremely detailed description of precisely what is 'unknown' about a given subsystem. Since the original problem arose because of a lack of detailed information about the properties of a subsystem, the problem becomes exacerbated and one is again forced to choose arbitrary values for missing information (in this case, the joint probability density function for the system).

It then becomes natural to question whether it is possible to adopt a statistical description of an uncertain subsystem which accounts for all information that is known about the subsystem, while minimizing the number of arbitrary assumptions that are made about the properties of the subsystem that are not known precisely. The current analysis provides one such description by assuming that: (i) the properties of the deterministic boundaries of the statistical subsystems are known precisely and (ii) the properties of the random boundaries of the statistical subsystems are known extremely imprecisely (or are extremely uncertain). The following sections discuss how such a subsystem may be included a vibro-acoustic analysis.

Consider the statistical subsystem illustrated in Fig. 7. In Ref. [11], it is shown that the response of a statistical subsystem with an uncertain boundary can be described in terms of the superposition of: (i) a direct field and (ii) a reverberant field. The direct field describes the outgoing displacement field associated with a prescribed displacement of the deterministic boundary, in the absence of the random boundary (as illustrated in Fig. 7a). The reverberant field satisfies: (i) a blocked (i.e., zero displacement) boundary condition across the deterministic boundary and (ii) the prescribed boundary condition across the random boundary, when added to the direct field. The direct field is independent of the properties of the random boundary; the reverberant field is extremely sensitive to the properties of the random boundary.

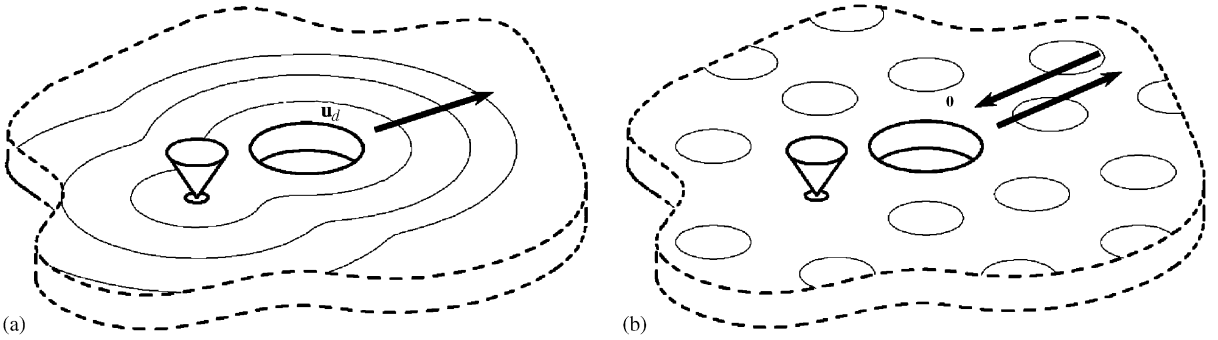

Fig. 7. Example of (a) direct field and (b) reverberant field of a connection to a statistical plate subsystem with deterministic boundary (solid line) and random boundary (dashed line). Gray lines indicate wavefronts in the direct field and local reactive energy flows in the reverberant field.

The uncoupled equations of motion for the mth statistical subsystem can be derived using a direct boundary element method and written as [11]

$$\mathbf{D}_{\mathrm{dir}}^{(m)}\mathbf{q} = \mathbf{f} + \mathbf{f}_{\mathrm{rev}}^{(m)}, \tag{2}$$

where $\mathbf{D}_{\mathrm{dir}}^{(m)}$ is the 'direct field dynamic stiffness' matrix for the mth statistical subsystem $\mathbf{f}$ is a vector of generalized forces and $\mathbf{f}_{\mathrm{rev}}^{(m)}$ is the blocked reverberant force on the connection degrees of freedom. The direct field dynamic stiffness matrix describes the force on the connection degrees of freedom due to the generation of a 'direct field' in the mth subsystem (in the absence of the random boundary). In general, this dynamic stiffness may be computed from a boundary element model; however, for simple point, line and area connections, the dynamic stiffness may also be estimated analytically (this point is discussed in more detail in subsequent sections). If the connection regions are assumed to be 'coherently coupled', then the calculation of the direct field dynamic stiffness matrix of a subsystem involves all connection regions. If the connection regions are assumed to be 'incoherently coupled', then the contribution to the direct field dynamic stiffness is found separately for each connection region.

The reverberant force $\mathbf{f}_{\mathrm{rev}}^{(m)}$ describes the force on the connection degrees of freedom arising from the reverberant field in the mth subsystem. As explained in Ref. [11], it represents a blocked force, i.e., the force acting when the connection degrees of freedom are held fixed.

2.4. Assembled equations of motion

Assembling the equations of motion for the statistical and deterministic subsystems in a system gives

$$\mathbf{D}_{\mathrm{tot}}\mathbf{q} = \mathbf{f}_{\mathrm{ext}} + \sum_{m} \mathbf{f}_{\mathrm{rev}}^{(m)}, \tag{3}$$

where $\mathbf{f}_{\mathrm{ext}}$ is the vector of generalized forces applied to the coupled system arising from external excitation, and where

$$\mathbf{D}_{\mathrm{tot}} = \mathbf{D}_{d} + \sum_{m} \mathbf{D}_{\mathrm{dir}}^{(m)}. \tag{4}$$

The total dynamic stiffness matrix for the system $\mathbf{D}_{\mathrm{tot}}$ is found by adding the dynamic stiffness of the deterministic subsystems to the direct field dynamic stiffness of the statistical subsystems. If there is uncertainty in the properties of the random boundaries of the statistical subsystems, then the blocked reverberant forces in Eq. (3) become random variables. Writing Eq. (3) in cross-spectral form and averaging over an ensemble of random boundaries gives

$$\langle \mathbf{S}_{qq} \rangle = \mathbf{D}_{\mathrm{tot}}^{-1} \langle \mathbf{S}_{ff} \rangle \mathbf{D}_{\mathrm{tot}}^{-\mathrm{H}}, \tag{5}$$

where $\langle . \rangle$ indicates an ensemble average and where the expected cross-spectrum of the blocked force is given by

$$\langle \mathbf{S}_{ff} \rangle = \mathbf{S}_{ff}^{\mathrm{ext}} + \sum_{m} \left(\mathbf{f}_{\mathrm{ext}} \langle \mathbf{f}_{\mathrm{rev}}^{(m),\mathrm{H}} \rangle + \langle \mathbf{f}_{\mathrm{rev}}^{(m)} \rangle \mathbf{f}^{\mathrm{H}} \right) + \sum_{m,n} \langle \mathbf{f}_{\mathrm{rev}}^{(m)} \mathbf{f}_{\mathrm{rev}}^{(n),\mathrm{H}} \rangle. \tag{6}$$

The symbol $.^{-\mathrm{H}}$ is used to denote the Hermitian transpose of the inverse of a matrix, so that $\mathbf{A}^{-\mathrm{H}}$ represents the following operations: conjugate(transpose(inverse($\mathbf{A}$))). The expected value of the

response clearly depends on the statistics of the blocked reverberant force. In turn, the statistics of the blocked reverberant force depend on the ensemble of random boundary curves assumed in a given analysis.

2.5. An ensemble of random boundaries

At first sight, it might appear that no meaningful statements can be made about the statistics of the blocked reverberant force without a more precise definition of the ensemble of random boundary curves assumed in a given analysis. However, specifying an ensemble implicitly defines some information about the random boundary. Of all possible ensemble definitions, there exists a unique ensemble that provides the minimum amount of information about the random boundary. This ensemble has the maximum uncertainty or maximum entropy of all possible ensembles. It can be shown [11] that as the amount of uncertainty regarding the properties of the random boundaries of the statistical subsystems increases, the blocked force in Eq. (6) tends to the following limit

$$\langle \mathbf{S}_{ff} \rangle = \mathbf{S}_{ff}^{\text{ext}} + \sum_m \mathbf{S}_{ff}^{(m),\text{rev}}, \tag{7}$$

where the cross-spectrum of the blocked reverberant force associated with the reverberant field of the mth subsystem is given by

$$\mathbf{S}_{ff}^{(m),\text{rev}} = \alpha_m \,\text{Im}\left\{\mathbf{D}_{\text{dir}}^{(m)}\right\}. \tag{8}$$

The constant of proportionality α_m is related to the (ensemble average) incident power in the reverberant field of the mth subsystem [11] (this constant is defined explicitly in subsequent derivation). Eqs. (7) and (8) represent a diffuse field reciprocity relationship between the direct field radiation from a connection to a statistical subsystem and the ensemble average blocked reverberant force on the connection. As discussed in Ref. [11], this relationship is a statistical property of an ensemble; it does not necessarily hold for individual realizations of the ensemble (although similar statistics are often observed when an average is taken over many local modes of a given subsystem). Furthermore, in this derivation, a 'diffuse' reverberant field is not an approximation made for analytical convenience, but rather it is a limiting statistical property that arises naturally when considering a large ensemble of random boundaries.

2.6. Ensemble average response

Inserting Eqs. (7) and (8) into Eq. (5) gives

$$\langle \mathbf{S}_{qq} \rangle = \mathbf{D}_{\text{tot}}^{-1} \left(\mathbf{S}_{ff}^{\text{ext}} + \sum_m \alpha_m \,\text{Im}\left\{\mathbf{D}_{\text{dir}}^{(m)}\right\} \right) \mathbf{D}_{\text{tot}}^{-\text{H}}. \tag{9}$$

Eq. (9) is an exact expression for the ensemble average response of a system of coupled subsystems with uncertain boundaries (that possess the statistics discussed previously). In order to solve Eq. (9), it is necessary to determine the (ensemble average) amplitudes α_m of the reverberant fields in the statistical subsystems. However, the amplitudes of the reverberant fields are functions of the

response $\langle \mathbf{S}_{qq} \rangle$; Eq. (9) does not therefore contain enough information for an explicit calculation of the response. The additional information that is needed to solve Eq. (9) is introduced by considering conservation of energy in the reverberant fields of the statistical subsystems, when averaged across the ensemble. The ensemble average amplitudes of the reverberant fields α_m can then be found by solving a set of linear simultaneous equations (similar in form to the symmetric SEA equations). The following sections derive the various expressions that are needed to form the power balance equations for the ensemble average response of the reverberant fields.

3. Ensemble average power in a reverberant field

3.1. Incident power and modal energy density

The ensemble average incident power in the reverberant field of the mth statistical subsystem can be defined in a number of ways. If the incident power is related to the expected energy density, group velocity and dimension of the subsystem, then it can be shown [11] that the constant α_m can be written as[3]

$$\alpha_m = \frac{4E_m}{\pi \omega n_m}, \tag{10}$$

where E_m is the total energy contained in the reverberant field of the mth subsystem, and n_m is the modal density of the mth subsystem. Explicit definitions for these quantities can be found in Ref. [11].

3.2. Power balance for mth reverberant field

Consider the ensemble average energy flows in the reverberant field of the mth statistical subsystem illustrated in Fig. 8. The input power to the reverberant field $P^{(m)}_{in,\mathrm{dir}}$ is due to energy in the direct field of the mth subsystem flowing across the random boundary. The power losses are due to: (i) dissipation within the reverberant field and (ii) the rate at which work is done on the connection degrees of freedom by the blocked reverberant force within the subsystem.[4] Applying conservation of energy to the steady-state response of the mth reverberant field results in the following power balance equation

$$P^{(m)}_{\mathrm{in,dir}} = P^{(m)}_{\mathrm{out,rev}} + P_{\mathrm{diss},m}. \tag{11}$$

[3]The definition of the incident power in the reverberant field of a subsystem in terms of a modal energy density is not essential, but simplifies the description of the dissipated power (in terms of a damping loss factor) and enables the current approach to be more readily compared with traditional SEA.

[4]Some of this energy is dissipated within the junctions (and deterministic subsystems) in the system, the remainder is transferred into the direct fields of any adjacent statistical subsystems.

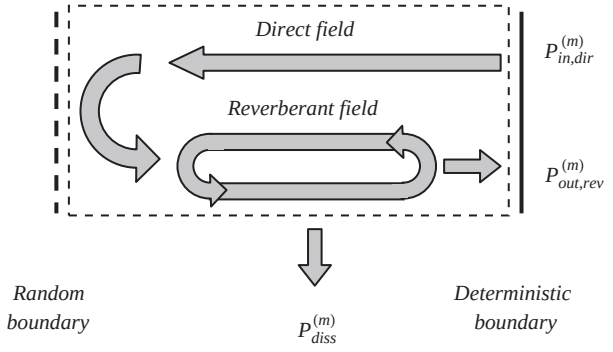

Fig. 8. Schematic representation of ensemble average energy flows within a statistical subsystem.

3.3. Input power to mth reverberant field

The time and ensemble average input power to the direct field of the mth statistical subsystem is given by

$$P^{(m)}_{\mathrm{in,dir}} = \frac{\omega}{2}\sum_{jk} \mathrm{Im}\left\{D^{(m)}_{\mathrm{dir},jk}\right\}\left\langle S_{qq,jk}\right\rangle, \tag{12}$$

In general, the cross-spectrum $\mathbf{S}_{qq}$ is complex Hermitian; however, the previous expression yields a real answer because of the symmetry of the direct field dynamic stiffness matrices. Inserting Eqs. (9) and (10) into Eq. (12) gives

$$P^{(m)}_{\mathrm{in,dir}} = P^{(m)}_{\mathrm{in},0} + \sum_{n} h_{nm}\frac{E_n}{n_n}, \tag{13}$$

where

$$P^{(m)}_{\mathrm{in},0} = \frac{\omega}{2}\sum_{jk} \mathrm{Im}\left\{D^{(m)}_{\mathrm{dir},jk}\right\}\left(\mathbf{D}^{-1}_{\mathrm{tot}}\mathbf{S}^{\mathrm{ext}}_{ff}\mathbf{D}^{-H}_{\mathrm{tot}}\right)_{jk}, \tag{14}$$

$$h_{nm} = \frac{2}{\pi}\sum_{jk} \mathrm{Im}\left\{D^{(m)}_{\mathrm{dir},jk}\right\}\left(\mathbf{D}^{-1}_{\mathrm{tot}}\,\mathrm{Im}\left\{\mathbf{D}^{(n)}_{\mathrm{dir}}\right\}\mathbf{D}^{-H}_{\mathrm{tot}}\right)_{jk}. \tag{15}$$

Eq. (13) indicates that the ensemble average input power to the direct field of the mth subsystem can be separated into the input powers due to: (i) external excitation and (ii) contributions from the reverberant loading associated with the reverberant fields of each statistical subsystem (including the mth). The coefficient h_{nm} gives the ensemble average input power to the direct field of the mth subsystem per unit modal energy density in the reverberant field of the nth subsystem. This coefficient has been referred to previously as a 'power transfer coefficient' [14]. A comparison with the definition of the CLF employed in traditional SEA reveals that[5]

$$h_{nm} = \omega n_n \eta_{nm}. \tag{16}$$

[5]Numerous authors have discussed whether h_{nm} or η_{nm} provides the most physical insight into the coupling between subsystems (see, for example, Newland [12], Lyon and Scharton [13] and Fahy [14]). The advantage of h_{nm} is that the coupling parameter is a local property of the junction (and does not depend on the extent of the subsystem), the

Eqs. (15) and (16) provide a general definition of the CLFs between statistical subsystems coupled by an arbitrary number of deterministic subsystems (regardless of the shape of the connection regions or the number of degrees of freedom used to describe the displacement field across each connection region). It should be noted that the CLF defined here accounts for damping in any intervening deterministic subsystems (in contrast to the CLFs employed in traditional SEA). In Appendix A, it is shown that the ensemble average power transfer coefficients are always symmetric regardless of the dissipation in the intervening subsystems so that $h_{nm} = h_{mn}$.

3.4. Power leaving mth reverberant field

The ensemble average rate at which energy leaves the reverberant field of the mth subsystem is given by

$$P_{\text{out,rev}}^{(m)} = \frac{\omega}{2} \sum_{jk} S_{qq,jk}^{(m),\text{rev}} \operatorname{Im}\{D_{\text{tot},jk}\} = \frac{E_m}{n_m} h_{\text{tot},m}, \tag{17}$$

where $\mathbf{S}_{qq}^{(m),\text{rev}}$ represents the component of the response due to excitation by the mth reverberant field and where

$$h_{\text{tot},m} = \frac{2}{\pi} \sum_{jk} \operatorname{Im}\{D_{\text{tot},jk}\} \left(\mathbf{D}_{\text{tot}}^{-1} \operatorname{Im}\left\{ \mathbf{D}_{\text{dir}}^{(m)} \right\} \mathbf{D}_{\text{tot}}^{-H} \right)_{jk}. \tag{18}$$

The power transfer coefficient $h_{\text{tot},m}$ describes the total energy leaving the mth reverberant field per unit modal energy density in the mth reverberant field. Eq. (17) can also be written in an alternative form by explicitly describing the power dissipated by damping within the deterministic subsystems. The resistive component of the total dynamic stiffness consists of contributions from the direct fields of the various statistical subsystems and the damping applied to the deterministic subsystems so that

$$\operatorname{Im}\{\mathbf{D}_{\text{tot}}\}_{jk} = \operatorname{Im}\{\mathbf{D}_d\}_{jk} + \sum_n \operatorname{Im}\left\{ \mathbf{D}_{\text{dir}}^{(n)} \right\}_{jk}, \tag{19}$$

Eq. (17) can therefore also be written as

$$P_{\text{out,rev}}^{(m)} = \frac{E_m}{n_m} \left(h_m^{\alpha} + \sum_n h_{nm} \right), \tag{20}$$

where the term h_m^{α} is given by

$$h_m^{\alpha} = \frac{2}{\pi} \sum_{jk} \operatorname{Im}\{\mathbf{D}_d\}_{jk} \left(\mathbf{D}_{\text{tot}}^{-1} \operatorname{Im}\left\{ \mathbf{D}_{\text{dir}}^{(m)} \right\} \mathbf{D}_{\text{tot}}^{-H} \right)_{jk}. \tag{21}$$

The term h_m^{α} indicates the power dissipated by the deterministic subsystems in the system per unit modal energy density in the mth reverberant field.

(*footnote continued*)
advantage of η_{nm} is that it enables coupling and dissipated powers to be readily compared. For the current analysis, either coefficient may be readily computed from the other.

3.5. Power dissipated within the mth reverberant field

The ensemble average power dissipated within the mth reverberant field can be described by a damping loss factor η_m so that

$$P_{\mathrm{diss},m} = \omega \eta_m E_m. \tag{22}$$

For consistency with previous notation, it is convenient to relate the dissipated power to the modal energy density so that

$$P_{\mathrm{diss},m} = M_m \frac{E_m}{n_m}, \tag{23}$$

where M_m represents the (half power bandwidth) modal overlap factor for the mth reverberant field and is given by

$$M_m = \omega n_m \eta_m. \tag{24}$$

3.6. Reverberant power balance

Inserting Eqs. (23), (17) and (13) into Eq. (11) gives the following expression for power balance within the mth reverberant field

$$\left(M_m + h_{\mathrm{tot},m}\right) \frac{E_m}{n_m} - \sum_n h_{mn} \frac{E_n}{n_n} = P_{\mathrm{in},0}^{(m)}. \tag{25}$$

Writing the power balance equations for each reverberant field in turn results in a set of simultaneous equations for the ensemble average response of the reverberant fields

$$\begin{bmatrix} M_1 + h_{\mathrm{tot},1} - h_{11} & \cdots & -h_{1m} \\ \vdots & \ddots & \\ -h_{m1} & & M_m + h_{\mathrm{tot},m} - h_{mm} \end{bmatrix} \begin{bmatrix} \dfrac{E_1}{n_1} \\ \vdots \\ \dfrac{E_m}{n_m} \end{bmatrix} = \begin{bmatrix} P_{\mathrm{in},0}^{(1)} \\ \vdots \\ P_{\mathrm{in},0}^{(m)} \end{bmatrix}. \tag{26}$$

From Eq. (20), the previous expression can also be written as

$$\begin{bmatrix} M_1 + h_1^{\alpha} + \sum\limits_{n \neq 1} h_{n1} & \cdots & -h_{1m} \\ \vdots & \ddots & \\ -h_{m1} & & M_m + h_m^{\alpha} + \sum\limits_{n \neq 1} h_{m1} \end{bmatrix} \begin{bmatrix} \dfrac{E_1}{n_1} \\ \vdots \\ \dfrac{E_m}{n_m} \end{bmatrix} = \begin{bmatrix} P_{\mathrm{in},0}^{(1)} \\ \vdots \\ P_{\mathrm{in},0}^{(m)} \end{bmatrix}. \tag{27}$$

If the deterministic subsystems are undamped (so that $h_m^{\alpha} = 0$ for all m), then the previous expression is identical to the symmetric form of the SEA equations [1,2]. However, in this derivation the equations arise by considering the ensemble average power balance between a set of coupled subsystems with uncertain boundaries. The current approach also provides an explicit definition of the CLFs (or power transfer coefficients) between all statistical subsystems regardless

of the level of deterministic detail introduced into the model. In general, the approach also automatically yields 'indirect' CLFs (CLFs between statistical subsystems that are not physically adjacent). If the modal overlap or absorption h_m^α is non-zero for each statistical subsystem, then the previous matrix is positive-definite and can be inverted to find the response of the reverberant fields of the statistical subsystems. The reverberant field response can then be inserted into Eq. (9) to find the ensemble average cross-spectral response of the system.

This concludes the derivation of the proposed method. The following sections summarize the solution procedure for the method and provide a numerical example.

4. Summary of the method

The solution procedure for the method derived in the previous sections is summarized below:

System definition

(i) A system is partitioned into a set of coupled subsystems. Connection regions are specified on each subsystem.
(ii) The deterministic boundaries of the various subsystems are then defined. This definition (along with the choice of substructuring and the definition of coherently coupled and incoherently coupled connection regions) explicitly defines the parts of a system that are assumed to be known deterministically. Typically, the identification of the deterministic boundary regions is based on an estimate of the propagating wavelengths within a given subsystem (in many instances this step may simply consist of a statement that subsystems smaller than a wavelength are modeled deterministically).
(iii) Degrees of freedom are specified for: (a) the deterministic subsystems and (b) the junctions which involve only statistical subsystems (the 'statistical junctions' in the system).

Assembly of direct field equations

(iv) The dynamic stiffness matrix for the deterministic subsystems $\mathbf{D}_d$ is obtained at a given frequency of interest using, for example, a finite or boundary element analysis. The excitation applied to the system is specified in terms of a cross-spectral matrix at a given frequency of interest $\mathbf{S}_{ff}^{\text{ext}}$.
(v) The direct field dynamic stiffness matrix $\mathbf{D}_{\text{dir}}^{(m)}$ is calculated for each statistical subsystem. In general, this dynamic stiffness can be found from a boundary element analysis of the deterministic boundaries of each statistical subsystem. However, in many instances the dynamic stiffness can also be found analytically for 'canonical' point, line and area connections to common subsystems (with the assumption that the response of distant connections to the same subsystem are incoherent). Such an approach results in significant savings in computational expense and is justified for connections whose separation is large (and/or uncertain) in comparison with a wavelength. It is noted in passing that this assumption is usually employed in the traditional wave approach to SEA (where CLFs are calculated locally for individual junctions).
(vi) The total dynamic stiffness matrix for the system is then assembled (Eq. (4)).

Assembly of reverberant field equations

(vii) The input power to each statistical subsystem due to the external excitation is calculated using Eq. (14).
(viii) The 'power transfer coefficients' (or CLFs) between the statistical subsystems are then calculated using Eq. (15) (looping over the excited and receiving statistical subsystems).
(ix) The 'total power transfer coefficients' are calculated for each statistical subsystem using Eq. (18).
(x) The modal overlap factors are calculated for each statistical subsystem using Eq. (24).
(xi) The reverberant power balance equations are assembled for the statistical subsystems using Eq. (26) and the external input powers found at step (vii).

Solution for reverberant response and direct field response

(xii) The reverberant power balance equations in Eq. (26) are solved to find the ensemble average modal energy density in the reverberant field of each statistical subsystem.
(xiii) The reverberant energy levels are inserted into Eqs. (9) and (10) to find the ensemble average cross-spectral response $\langle \mathbf{S}_{qq} \rangle$. The response consists of contributions from the external loading and the reverberant loading from each statistical subsystem.
(xiv) The total energy of each statistical subsystem is found by adding the energy in the direct and reverberant fields (in many instances, the former is small compared with the latter and can be neglected).
(xv) The analysis is repeated for each discrete frequency of interest.

5. Numerical example

The following section provides a simple numerical example in which predictions using the proposed method are compared with the results of a large FE Monte Carlo simulation. In this section, the proposed method is referred to as a 'Hybrid FE-SEA method' since the method combines deterministic and statistical (SEA-like) descriptions of the dynamic behavior of various subsystems in a system (although one could perhaps also view the method as being a generalized wave or boundary approach to SEA).

Consider the structure illustrated in Fig. 9. Two thin aluminum plates are connected to a z-section frame via five point connections; the first plate is excited and interest lies in predicting the transverse response of the second plate across a frequency range from 15 Hz to 1.5 kHz. The first plate is assumed to be excited by a transverse point force whose precise location within the subsystem is unknown; for a deterministic FE model, such an excitation can be represented by spatially incoherent (rain-on-the-roof) excitation. The properties of the structure are listed in Table 1. The structure has approximately 150 modes below 1.5 kHz. The chosen example has a relatively small number of modes compared with many vibro-acoustic problems of practical interest. For example, a typical vibro-acoustic model of a 2 m section of an aircraft fuselage can contain upwards of 400,000 structural modes below 10 kHz; the addition of internal acoustic

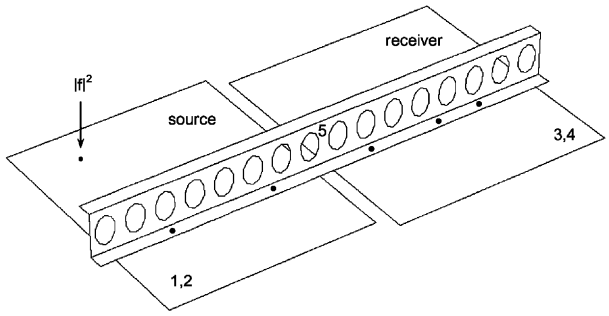

Fig. 9. A 'complex' structural system consisting of two statistical subsystems (the flexural wavefields of the two plates) point connected to various deterministic subsystems (the z-section frame and the in-plane wavefields of the two plates). Subsystem labels are discussed in Section 5.2.1.

Table 1
Properties of structure

Property	Value
Source plate thickness	1e−3 m
Receiving plate thickness	0.75e−3 m
Source plate dimension	0.28×0.35 m
Receiving plate dimension	0.3×0.35 m
Frame plate thickness	3e−3 m
Frame height	60e−3 m
Frame flange width	20e−3 m
Young's modulus	71e9 Pa
Poisson's ratio	0.33
Density	2700 kg/m^3
Damping Loss factor	0.01
Radius of point connections	5e−3 m

cavities to such a model increases the mode count to approximately 8 million modes below 10 kHz. The use of a smaller simplified numerical example (for which an FE Monte Carlo simulation is computationally tractable) has been adopted here to illustrate the general principles behind the Hybrid method. It is important to bear in mind, however, that, for most practical mid- and high-frequency vibro-acoustic problems, a statistical description of the complex subsystems in a system is essential in order to provide an analysis that is robust and computationally tractable.

The flexural wavefields of the plates are below modal overlap across the frequency range of interest (the half power modal overlap of the source plate equals unity at 3.20 kHz, while the half power modal overlap of the receiving plate equals unity at 2.24 kHz). The structure can be considered to be 'complex' since, across the frequency range of interest, the flexural wavelengths of the two plates are small in comparison with the dimension of the plates. An analysis of the vibro-acoustic behavior of the entire structure using traditional SEA is complicated by the

presence of various 'stiff' subsystems (the in-plane response of the plates and the z-section frame) and the nature of the connections between the subsystems (which are not particularly amenable to analysis using existing CLF formulations). An analysis of the vibro-acoustic behavior of the entire structure using FE is complicated by the sensitivity of the response to small perturbations in the properties of the structure (and, for more general structures, by the computational expense required to model the statistical subsystems with FE).

5.1. FE Monte Carlo simulation

An FE Monte Carlo simulation was performed in order to provide a comparison with the Hybrid method. Such an analysis requires that the ensemble of structures under consideration be defined precisely. There are various ways in which one might choose to define such an ensemble and at first sight it might appear that the choice of a particular ensemble is somewhat arbitrary. However, as discussed previously, the ensemble average response tends to become insensitive to the precise details of the ensemble as the amount of uncertainty is increased (the statistics quickly become saturated and tend to the maximum entropy limit). This therefore provides some motivation for adopting an ensemble in the current example that is simple to implement numerically. An ensemble was therefore generated by adding 20 point masses (each with a mass of 15 g) to the plates at random locations. It should be noted that the maximum entropy ensemble assumed in the Hybrid method encompasses such an ensemble (the random boundary for such an ensemble consists of a series of internal discontinuities with a particular reactive impedance).

The uncertainty introduced into the model in this example represents uncertainty in the distribution of approximately 25% of the mass of the structure. The amount of uncertainty was chosen to ensure that the lower-order modes of the plates were sufficiently perturbed across the ensemble (the higher-order modes of the plates are much more sensitive to perturbation and similar results can be obtained using significantly less added mass). The amount of uncertainty in the present example is not, however, unrealistic and provides perturbations similar to those that occur when there is uncertainty regarding the precise impedance boundary conditions of the plates.

An FE model of the (unperturbed) structure was created using approximately 5250 (CTRIA3) shell elements.[6] The resulting model contained approximately 15,000 analysis degrees of freedom. An eigensolution was then performed and 287 modes were extracted with natural frequencies below 3250 Hz. Fig. 10 shows an example mode shape with a natural frequency around 900 Hz. In order to reduce the computational expense of the Monte Carlo simulation, the global mode shapes were then used as basis functions in subsequent analysis. For each trial in the Monte Carlo simulation the impedance of the random point masses was projected onto the modal basis and (modal) mass and stiffness matrices were generated. A subsequent eigenproblem was then performed to obtain the modes and natural frequencies of the perturbed structure. The flexural energy in each plate subsystem, due to rain-on-the-roof excitation applied to the source plate, was calculated using the FE post-processing equations derived in Ref. [16].

[6]Such elements can be prone to locking [15]; the use of such elements is, however, not expected to alter the conclusions of the example.

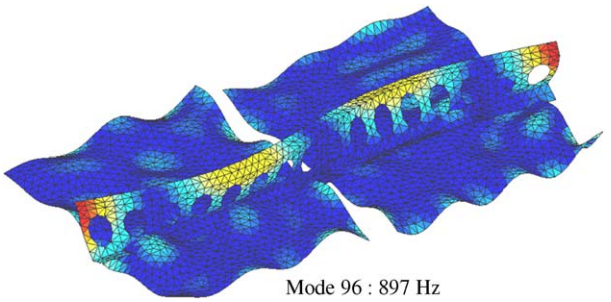

Fig. 10. Example of mode shape from a full FE model for a single realization of the ensemble.

The computed energies and input powers were used to build up an energy influence coefficient (EIC) matrix (the *ij*th entry of this matrix gives the energy in the *i*th subsystem due to input power applied to the *j*th subsystem). By examining the inverse of this matrix, it is possible to estimate the effective CLFs between various FE subsystems in a system for each realization of the ensemble. Ensemble average effective CLFs computed using the FE Monte Carlo simulation can then be compared with the ensemble average CLFs computed using the Hybrid approach.

The flexural energy in the receiving plate per unit input power to the source plate is plotted in Fig. 11 for two realizations of the ensemble. The sensitivity of the response to small changes in the properties of the two plates is clearly evident. For each realization of the ensemble, the 2×2 matrix of EICs was computed and inverted to obtain estimates of the 'effective CLFs' between the flexural wavefields of the two plate subsystems. The Monte Carlo simulation was performed for 500 separate realizations of the ensemble. The overall simulation took approximately 12 h on a 2 GHz desktop PC (it is noted in passing that the same simulation using a nodal basis rather than a modal basis would require approximately 120 h of simulation time).

The energy responses in the source and receiving subsystems are shown in Fig. 12 for each member of the ensemble. The variance in the response is clearly evident, even at relatively low frequencies. The ensemble average response is also plotted in the Figure. It can be seen that distinct fluctuations remain in the ensemble average response of the structure. For example, around 950 Hz a significant amount of energy is transmitted through the frame into the receiving plate across the ensemble (the peak response being approximately 10 dB higher than the response at neighboring frequencies). The increase of energy in the receiving plate is accompanied by a slight reduction in the energy of the source plate (approximately 2–3 dB at 950 Hz). The effective CLFs between the flexural wavefields of the two plate subsystems, calculated using the Monte Carlo simulation, are plotted in Fig. 13. Similar fluctuations are observed in the effective CLF when averaged across the ensemble (although such fluctuations are difficult to discern from an examination of the effective CLF of a given realization of the ensemble).

5.2. *Hybrid method*

This section discusses the creation of a Hybrid model of the example structure. To illustrate the general approach, the solution procedure described in Section 4 is followed.

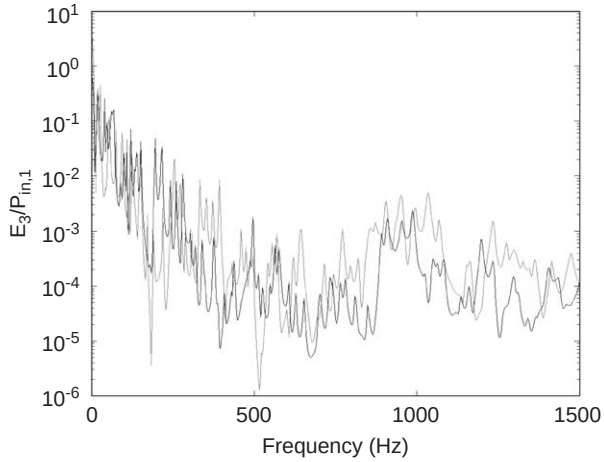

Fig. 11. Flexural energy in receiving plate per unit input power applied to source plate, computed using full FE model. Comparison of response obtained for two separate realizations of the ensemble.

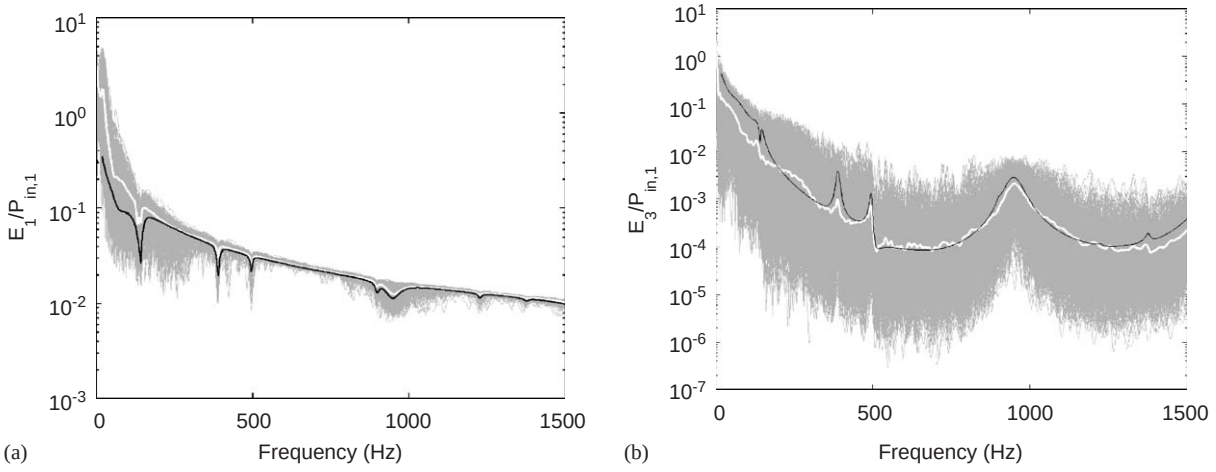

Fig. 12. Energy in flexural wavefields of (a) source plate and (b) receiving plate, per unit input power computed using: (i) an FE Monte Carlo simulation and (ii) the Hybrid approach. Gray lines, computed using Monte Carlo approach for 500 realizations of ensemble; white line, ensemble average of FE results; black line, ensemble average computed using Hybrid approach.

5.2.1. System definition

The classification of the subsystems in a system into statistical and deterministic subsystems can be based on an approximate estimate of the number of half wavelengths within the various subsystems across a given frequency range of interest. Table 2 lists the number of expected half wavelengths within the plate subsystems (estimated from the free wavenumber within these subsystems). It can be seen that, for this structure, the flexural wavefields of the plates are likely to be well represented by statistical subsystems across the frequency range of interest, while the in-plane wavefields are likely to well represented by deterministic subsystems. The frame subsystem is

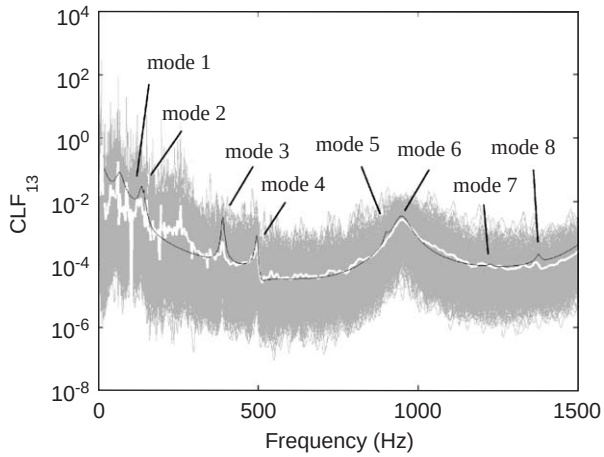

Fig. 13. CLF between flexural wavefields of plates computed using: (i) an FE Monte Carlo simulation and (ii) the Hybrid approach. Gray lines, CLFs computed using Monte Carlo approach for 500 realizations of ensemble; white line, ensemble average of FE results; black line, CLF computed using Hybrid approach. Peaks in CLF associated with global basis functions of FE subsystems (mode number labeled).

Table 2
Classification of plate subsystems used in model

Subsystem	Description	ka/π at 15 Hz	ka/π at 1.5 kHz	Classification
1	Plate flexural wavefield	0.8	8	Statistical
2	Plate in-plane wavefield	0.03	0.3	Deterministic
3	Plate flexural wavefield	0.9	9	Statistical
4	Plate in-plane wavefield	0.03	0.3	Deterministic

relatively stiff and has few modes across the frequency range of interest and is therefore likely to be well represented by a deterministic subsystem.

The connection regions for the statistical subsystems are defined by the locations of the point connections to the frame and the locations of the applied excitation. The excited plate contains three point connections (two associated with junctions and one associated with the location of the excitation). The deterministic boundary for the statistical subsystems is defined by the location of the connection regions (it is noted in passing that if additional boundary conditions were present in the vicinity of the connections then these could be included in the analysis). The deterministic boundary is defined so that the connection regions are internal to each statistical subsystem.

In this example, the degrees of freedom for the Hybrid model are taken to be the modal degrees of freedom of the deterministic subsystems. The degrees of freedom for the connection to the excitation in the excited subsystem are taken to be the six physical degrees of freedom associated with a point connection (this is explained in more detail in subsequent discussion). A finite element model of the deterministic subsystems (the frame and in-plane response of the plates) was created by replacing the shell elements in the plate subsystems of the FE model of the previous

section with membrane elements (CTRMEM). To ensure that the FE model only accounted for the in-plane mass of the plate subsystems (and not the transverse mass), the mass of the membrane elements was applied separately (by directly specifying concentrated masses applied to the in-plane degrees of freedom). A modal analysis was then performed on the FE subsystems and 29 mode shapes were extracted with frequencies below 3250 Hz (compare this with the FE model of the previous section in which approximately 290 modes were extracted over the same frequency range). By definition, the deterministic subsystems in a Hybrid model contain relatively few modes, and the resulting eigenproblem is therefore numerically efficient.

5.2.2. Assembly of direct field equations

The deterministic dynamic stiffness matrix for the system is found from the dynamic stiffness of the global basis functions. The local direct field dynamic stiffness matrix $\mathbf{D}_{\mathrm{dir}}^{(m)}$ for each statistical subsystem can, in general, be computed from a boundary element analysis. Such an approach accounts for the coherence that occurs between the various connections to a subsystem. However, in many instances it is often acceptable to neglect the coherence that occurs between the various connections and consider the direct field dynamic stiffness of each connection in isolation. Such an approach is computationally efficient and is justified if there is uncertainty in the relative spacing of the connections (or if the spacing between the connections is large in comparison with a wavelength). In this example, the various connection regions to the statistical subsystems were therefore assumed to be 'incoherently coupled'. Neglecting the coherence between the excitation and junction connection regions therefore implicitly accounts for the uncertainty in the precise location of the excitation connection region within the excited subsystem (this can be viewed as being equivalent to applying rain-on-the-roof-excitation to the excited subsystem).

The direct field dynamic stiffness of each connection region can then be obtained using a wave analysis [9]. In this approach, the direct field dynamic stiffness of each point connection corresponds to the dynamic stiffness of a rigid disk embedded in an infinite plate (the current analysis only requires the contributions to the dynamic stiffness arising from flexural waves). The dynamic stiffness of each point connection is then projected onto the global basis functions to obtain the contribution to the direct field dynamic stiffness matrix from each statistical subsystem $\mathbf{D}_{\mathrm{dir}}^{(m)}$.

The total dynamic stiffness matrix for the system is then assembled and the input power due to the externally applied excitation is found (in this example, since the coherence between the various point connections is neglected, the input power to the source subsystem is equivalent to the input power to an infinite plate). The power transfer coefficients are then calculated for the statistical subsystems using Eqs. (15) and (18), and the reverberant power balance equations assembled (in this example, the reverberant power balance matrix is of dimension 2×2). The calculation of the modal overlap of each statistical subsystem requires that the modal densities of the statistical subsystems be known; in this example the modal densities were calculated using standard expressions [9].

5.2.3. Solution for reverberant response and response recovery

The reverberant power balance matrix can then be inverted and the reverberant response of each statistical subsystem obtained. Since the plate subsystems are lightly damped, the total energy of the plate is likely to be dominated by the reverberant field and the contribution to the

total energy from the direct field was therefore neglected in this example. The response calculation was repeated for 1000 frequency points of interest. The entire calculation took less than a minute (compare this with the 12 or 120 h Monte Carlo simulations discussed in the previous section).

The Hybrid prediction of the ensemble average energy in the source and receiving plates is overlaid in Fig. 12. There is reasonably good agreement between the Hybrid prediction and the results of the Monte Carlo simulation. The discrepancies between the two results at lower frequencies are most likely due to the limited amount of uncertainty in the properties of the plates in the Monte Carlo simulation (closer agreement might be expected if the size and shapes of the plates are also perturbed in the Monte Carlo simulation in order to increase the amount of uncertainty in the ensemble). Some discrepancies may also be due to convergence issues (due to the finite number of trials in the Monte Carlo simulations and the finite number of basis functions used in the Monte Carlo and Hybrid analyses).

The CLF between the source and excited wavefields computed using the Hybrid approach is plotted in Fig. 13. There is good agreement between this CLF and the ensemble average of the effective CLFs obtained in the Monte Carlo simulation. However, the Hybrid approach also provides insights into the way in which energy is transmitted between the source and receiving plates across the ensemble. Each peak in the predicted CLF corresponds to a particular global basis function of the deterministic subsystems. The various global basis functions have been labeled in the figure (nb. six rigid body basis functions were also included in the analysis but are not labeled). Each global basis function of the deterministic subsystems provides a separate transmission path between the statistical subsystems. Indeed, the deterministic subsystems can be viewed as extended dissipative junctions which couple the various statistical subsystems in a model.

By restricting the number of degrees of freedom used in the Hybrid analysis, it is possible to perform an approximate contribution analysis to estimate how each global basis function contributes to a given CLF. The contribution to the CLF from the various global basis functions of the deterministic subsystems is plotted in Fig. 14. It can be seen that the peak that occurs in the ensemble average CLF around 950 Hz is primarily due to the contribution of a single global basis function (the sixth global basis function). Examples of the various global basis functions used in the Hybrid model are illustrated in Fig. 15. It can be seen that the sixth global basis function provides a particularly good transmission path because of the spatial matching that occurs between the mode shape and the connection locations (the mode shape has a large displacement at the various connection points).

The transmission of energy between the two statistical subsystems can be modified by modifying the contributions to the overall CLF from the various global basis functions. For example, one strategy for reducing the ensemble average transmission around 950 Hz is to investigate the use of alterative locations for the point connections to the frame. Since the Hybrid model is computationally efficient, the effects of design changes on the transmission of energy between the statistical subsystems can be readily evaluated and robust design changes (design changes that are insensitive to perturbation) can be identified. For example, the effects of isolators, alternative frame designs and localized damping treatments can be readily evaluated.

To demonstrate this, Fig. 16 shows the effect that the addition of a local damping treatment to the FE subsystems has on the computed CLF (in this example, the damping loss factor of the FE subsystems was modified from 0.01 to 0.1, to model, for example, the addition of a viscoelastic

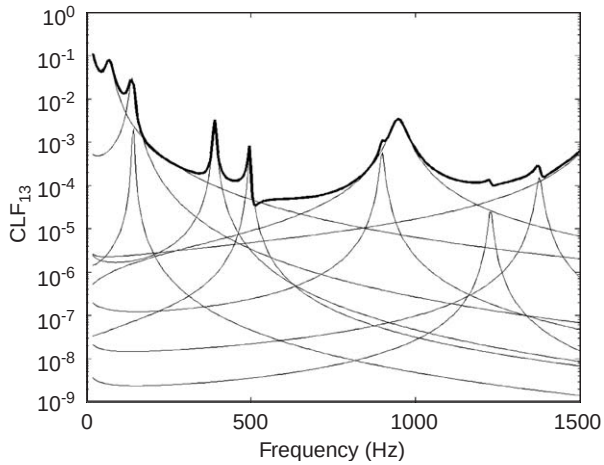

Fig. 14. Contribution to CLF from various global basis functions of deterministic subsystems computed using Hybrid approach: thick line, total CLF computed using all global basis functions; thin lines, CLF computed when analysis only includes a particular global basis function.

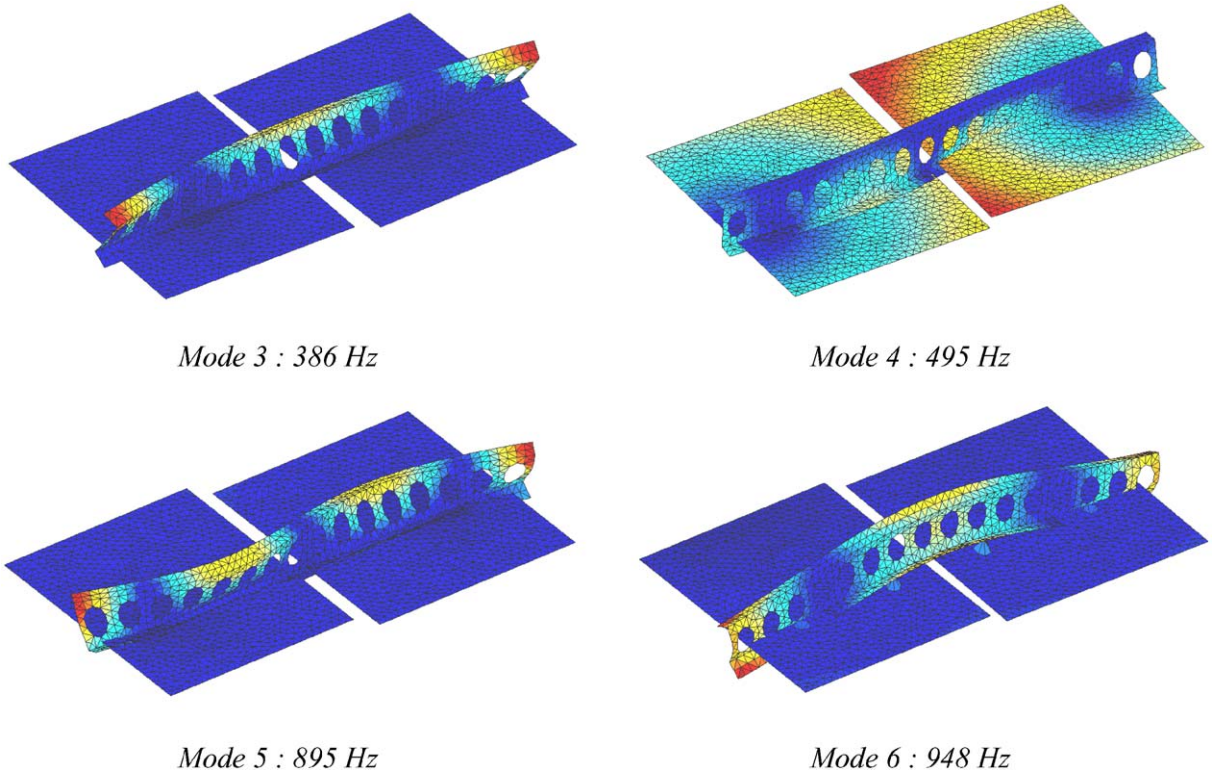

Fig. 15. Examples of global basis functions used in the Hybrid model (nb. plots only include contributions from membrane motion when plotting the response of the plate subsystems).

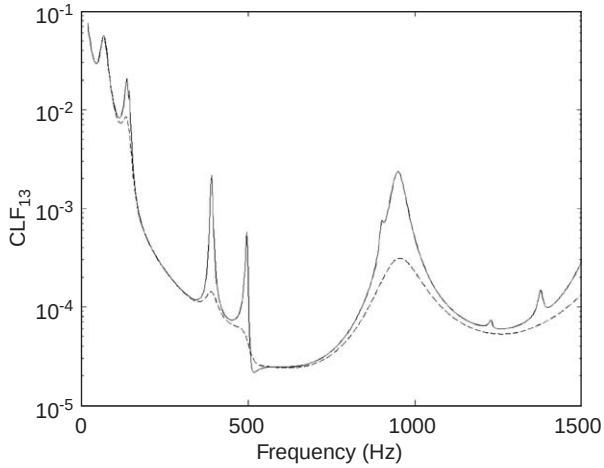

Fig. 16. Effect of modification to damping loss factor of FE subsystems on CLF between flexural wavefields of plates (calculated using Hybrid approach): solid line, $\eta_{FE} = 0.01$; dashed line, $\eta_{FE} = 0.1$).

damping treatment to the frame). It can be seen that the increased damping has most influence at the resonances of the FE subsystems (and has relatively little influence when the transmission is dominated by the non-resonant response of the frame). In this example, the additional damping reduces the ensemble average CLF by approximately 10 dB around 950 Hz.

A Hybrid model also has potential application for the design of robust broadband active noise control systems. In such applications an active control system may be designed to target the global basis functions of the deterministic subsystems in a system, in order to minimize the transmission of vibrational energy through a complex system. A Hybrid model provides an efficient means with which to evaluate the effectiveness of such control schemes, and provides insights into where to locate actuators and sensors in order to improve control performance.

It is sometimes stated that a necessary requirement for the application of SEA methods is that the modal overlap in the statistical subsystems be greater than unity. As can be seen in the previous example, this statement is not strictly correct. A modal overlap greater than unity reduces the variance of the response across the ensemble (and ensures that the response of a single realization of the ensemble is more likely to match the ensemble average response), but is not necessarily a prerequisite for the successful application of SEA methods (the modal overlap of the source plate in this example equals unity at 3.20 kHz, while the modal overlap of the receiving plate equals unity at 2.24 kHz).

6. Concluding remarks

A general method has been presented for predicting the ensemble average response of coupled subsystems with uncertain properties. The method has been derived explicitly without reference to existing derivations of SEA; however, the traditional wave approach to SEA can be viewed as a special case of the proposed method. The advantage of the proposed method is that it provides a

systematic way to analyze the response of systems that are not particularly amenable to analysis by existing SEA (or FE) methods. In particular, the proposed method enables an arbitrary amount of deterministic detail to be included in a given analysis (without requiring that an entire system be known deterministically). The deterministic subsystems in a system can be viewed as spatially distributed 'lossy' junctions that transfer energy between the statistical subsystems in a system (these junctions may also be directly excited in the proposed approach).

There are a number of philosophical differences between the proposed method and traditional SEA that warrant further discussion. In the current derivation, the proposed method has been presented as an analytically exact statistical method (approximations may be introduced when estimating the direct field dynamic stiffness of a subsystem; however, the underlying method is exact). No assumptions were made regarding the strength of coupling between subsystems, the nature of the excitation or the resonant nature of the response. Such assumptions were instead replaced with the assertion that a significant amount of uncertainty exists regarding the properties of certain subsystems. Defining the deterministic boundaries (and subsystems) of a system therefore implicitly defines the ensemble in the current analysis.

The value of this approach depends on how well the assumed ensemble matches the ensembles encountered in practical applications. Since detailed information about the sources of uncertainty in complex structures is seldom available (and in most practical instances is seldom attainable), the proposed approach represents a compromise in which the information that is precisely known about a system can be included in an analysis while minimizing the assumptions made about missing information. For many practical applications, the definition of the deterministic and statistical portions of a model can often be made based on estimates of the propagating wavelengths within various regions of a system. Since the wavelengths within typical subsystems can often differ by several orders of magnitude, an order of magnitude estimate of the wavelength in comparison with the subsystem dimension is often all that is required.

In traditional SEA it is sometimes assumed that, since the modal density is an input quantity, the size of an SEA subsystem is assumed to be deterministic. In the current analysis, the responses of the reverberant fields are determined from a power balance rather than an energy balance (the modal density is a secondary quantity that is used to relate the incident power in a reverberant field to the total energy of the reverberant field). Interestingly, in the current analysis, the size of a statistical subsystem is therefore not a required input quantity (the size of a statistical subsystem enters the analysis indirectly through the definition of the power dissipated within the reverberant field of the subsystem). The minimum amount of information that is needed to model the ensemble average response of a statistical subsystem in the proposed method is: (i) the direct field dynamic stiffness of the connections to the subsystem and (ii) the modal overlap of the subsystem.

Finally, it should be noted that the discussion in the current manuscript has been restricted to estimates of the ensemble average response. The extension of the method to encompass higher order response statistics is the subject of ongoing research.

Acknowledgements

The authors would like to acknowledge the support of Paul Bremner, without whom this work would not have been possible. Helpful discussions with Bryce Gardner and Vincent Cotoni are

also gratefully acknowledged. This work has been funded by Vibro-Acoustic Sciences Inc. Commercial software implementation of the method described in this paper is subject to US Patent 6,090,147.

Appendix A

In this appendix, it is demonstrated that the matrix of power transfer coefficients is symmetric for a linear system so that $h_{nm} = h_{mn}$. From Eq. (15), the nmth power transfer coefficient is given by

$$h_{nm} = \frac{2}{\pi} \sum_{jk} \mathrm{Im}\left\{\mathbf{D}_{\mathrm{dir}}^{(m)}\right\}_{jk} \left(\mathbf{D}_{\mathrm{tot}}^{-1} \mathrm{Im}\left\{\mathbf{D}_{\mathrm{dir}}^{(n)}\right\} \mathbf{D}_{\mathrm{tot}}^{-H}\right)_{jk}. \tag{28}$$

Writing the matrix multiplication as a summation gives

$$h_{nm} = \frac{2}{\pi} \sum_{jkrs} \mathrm{Im}\left\{\mathbf{D}_{\mathrm{dir}}^{(m)}\right\}_{jk} \mathrm{Im}\left\{\mathbf{D}_{\mathrm{dir}}^{(n)}\right\}_{rs} \left(\mathbf{D}_{\mathrm{tot}}^{-1}\right)_{jr} \left(\mathbf{D}_{\mathrm{tot}}^{-H}\right)_{sk}. \tag{29}$$

The mnth power transfer coefficient is given by

$$h_{mn} = \frac{2}{\pi} \sum_{jkrs} \mathrm{Im}\left\{\mathbf{D}_{\mathrm{dir}}^{(m)}\right\}_{jk} \mathrm{Im}\left\{\mathbf{D}_{\mathrm{dir}}^{(n)}\right\}_{rs} \left(\mathbf{D}_{\mathrm{tot}}^{-1}\right)_{rj} \left(\mathbf{D}_{\mathrm{tot}}^{-H}\right)_{ks}. \tag{30}$$

The receptance matrix of a linear system described by real basis functions can always be written in a symmetric form so that

$$\left(\mathbf{D}_{\mathrm{tot}}^{-1}\right)_{jr} = \left(\mathbf{D}_{\mathrm{tot}}^{-1}\right)_{rj}, \quad \left(\mathbf{D}_{\mathrm{tot}}^{-H}\right)_{sk} = \left(\mathbf{D}_{\mathrm{tot}}^{-H}\right)_{ks}. \tag{31}$$

Inserting the previous expression into Eq. (30) gives

$$h_{mn} = \frac{2}{\pi} \sum_{jkrs} \mathrm{Im}\left\{\mathbf{D}_{\mathrm{dir}}^{(m)}\right\}_{jk} \mathrm{Im}\left\{\mathbf{D}_{\mathrm{dir}}^{(n)}\right\}_{rs} \left(\mathbf{D}_{\mathrm{tot}}^{-1}\right)_{jr} \left(\mathbf{D}_{\mathrm{tot}}^{-H}\right)_{sk} = h_{nm}. \tag{32}$$

This therefore provides the required demonstration of the symmetry of the power transfer coefficient matrix. It should be noted that the power transfer coefficients defined here describe the ensemble average energy flow in a system (the previous result is therefore a relationship which holds for the ensemble but not necessarily for any given realization).

References

[1] R. Lyon, *Statistical Energy Analysis of Dynamical Systems*, MIT Press, Cambridge, MA, 1975.
[2] F. Fahy, Statistical energy analysis: a critical overview, *Philosophical Transactions of the Royal Society of London A* 346 (1994) 431–447.
[3] R. Lyon, Statistical energy analysis and structural fuzzy, *Journal of the Acoustical Society of America* 97 (5) (1995) 2878–2881.
[4] R. Lyon, E. Eichler, Random vibration of connected structures, *Journal of the Acoustical Society of America* 36 (7) (1964) 1344–1354.

[5] M. Heckl, Measurement of absorption coefficients on plates, *Journal of the Acoustical Society of America* 34 (6) (1962) 803–808.
[6] R. Langley, K. Heron, Elastic wave transmission through plate/beam junctions, *Journal of Sound and Vibration* 143 (2) (1990) 241–253.
[7] I. Bosmans, T. Nightingale, Modeling vibrational energy transmission at bolted junctions between a plate and a stiffening rib, *Journal of the Acoustical Society of America* 109 (3) (2001) 999–1010.
[8] R. Langley, P. Shorter, Diffuse wavefields in cylindrical coordinates, *Journal of the Acoustical Society of America* 112 (4) (2002) 1465–1470.
[9] R. Langley, P. Shorter, The wave transmission coefficients and coupling loss factors of point connected structures, *Journal of the Acoustical Society of America* 113 (4) (2003) 1947–1964.
[10] B. Mace, Wave coherence, coupling power and statistical energy analysis, *Journal of Sound and Vibration* 199 (3) (1997) 369–380.
[11] P. Shorter, R. Langley, On the reciprocity relationship between direct field radiation and diffuse reverberant loading, *Journal of the Acoustical Society of America* 117 (1) (2005) 85–95.
[12] D. Newland, Comment on 'Vibrational-Energy Transmission in a three-element structure', *Journal of the Acoustical Society of America* 39 (4) (1966) 755.
[13] R. Lyon, T. Scharton, Reply to Comment on 'Vibrational-Energy Transmission in a three-element structure', *Journal of the Acoustical Society of America* 39 (4) (1966) 755–756.
[14] F. Fahy, An alternative to the SEA coupling loss factor: Rationale and method for experimental determination, *Journal of Sound and Vibration* 214 (2) (1998) 261–267.
[15] R. Macneal, *Finite Elements: Their Design and Performance*, Marcel-Dekker, New York, 1994.
[16] B. Mace, P. Shorter, Energy flow models from finite element analysis, *Journal of Sound and Vibration* 233 (3) (2000) 369–389.